Available online at www.sciencedirect.com
SCIENCE DIRECT
Thermochimica Acta 429 (2005) 31–42
thermochimica acta
www.elsevier.com/locate/tca

Thermal kinetic TG-analysis of the mixed-ligand copper(II) and nickel(II) complexes of *N*-(1-phenyl-3-methyl-4-benzylidene-5-pyrazolone) *p*-nitrobezoylhydrazide and pyridine

Guan-Cheng Xu, Li Zhang, Lang Liu, Guang-Fei Liu, Dian-Zeng Jia*

Institute of Applied Chemistry, Xinjiang University, Urumqi, 830046, PR China

Received 1 August 2004; received in revised form 1 November 2004; accepted 22 November 2004
Available online 29 December 2004

Abstract

Thermal behaviors of three mixed-ligand complexes, [Ni(PMBP-PNH)$(Py)_3$], [Ni(PMBP-PNH)Py] and [Cu(PMBP-PNH)Py] (PMBP-PNH = *N*-(1-phenyl-3-methyl-4-benzylidene-5-pyrazolone) *p*-nitrobezoylhydrazide; Py = pyridine), were studied by TG and DTG in dynamic air atmosphere. The complexes show the loss of pyridine molecule which is followed by the decomposition of the PMBP-PNH anion and give respective metal oxides as residues. Meanwhile, the Ozawa-Flynn-Wall model-free analyses and multivariate non-linear regression were applied to perform single and overall steps optimization. Kinetic parameters were given and the most probable mechanism functions were suggested in this study.

Keywords: Thermal analyses; Kinetic studies; Non-linear regression; Mixed-ligand complexes

1. Introduction

Pyrazolone-5, especially 4-acyl pyrazolones, form an important class of organic compounds and widely used in biological, analytical applications, catalysis and extraction metallurgy [1–5]. Furthermore, 4-acyl pyrazolone derivatives have a potential to form different types of coordination compounds due to the several electron-rich donor centers [6–9] and tautomeric effect of enol form and keto form [10–12]. Meanwhile, compounds containing hydrazide moieties and their complexes also possess biological activities, especially serving as potential inhibitors for many enzymes [13–15].

During the course of our research, we have synthesized a series of 4-acyl pyrazolone derivatives [16–18] and reported several transition metal complexes [19–22], but no detailed studies on thermal degradation and thermal kinetics have been carried out so far. Hence, As a continuation of our earlier study and the interest on the thermal properties of mixed-ligand complexes, we report in this paper the phenomenological, kinetic and mechanistic aspects of thermal decomposition of the nickel(II), copper(II) complexes of PMBP-PNH and containing pyridine as co-ligand.

2. Experimental

2.1. Reagents

The ligand PMBP-PNH was synthesized according to the procedure described in the literature [23]. Other chemicals and solvents were analytical grade and commercially available.

2.2. Instrumental

Elemental analyses of C, H and N were performed using a PE-2400C analyzer. Thermogravimetric measurements were carried out on a Netzsch STA 449C Model instrument. An alumina crucible was used in dynamic air

* Corresponding author. Tel.: +86 991 8580032; fax: +86 991 8581006.
E-mail address: jdz@xju.edu.cn (D.-Z. Jia).

0040-6031/$ – see front matter © 2004 Elsevier B.V. All rights reserved.
doi:10.1016/j.tca.2004.11.027

atmosphere (30 $cm^3\ min^{-1}$). The rate of heating was 20, 10 and 5 °C min^{-1} and sensitivity of the instruments is 0.1 μg. The crystal structure was determined by a Siemens P4 diffractometer and SHELXTL-97 crystallographic software package of molecular structure.

2.3. Syntheses of the complexes

The mixed-ligand complexes were synthesized using solvothermal method. The synthetical procedure of [Ni(PMBP-PNH)$(Py)_3$] [22] is as follows:

Equimolar PMBP-PNH and $Ni(Ac)_2{\cdot}4H_2O$ were grinded evenly and dissolved by moderate methanol. The clear solution was then removed in a Teflon bomb, adding 1 ml acetonitrile and 1 ml pyridine into the mixture. The bomb was heated to 120 °C and maintained at this temperature for 2 days. After slowly cooling down to the room temperature, the red-black block crystals were collected by filtration and dried in air.

The [Cu(PMBP-PNH)Py] was synthesized in the same condition. However, an interesting aspect of the experiments is that [Ni(PMBP-PNH)Py] was obtained when the reaction temperature is maintained at 150 °C.

2.4. The theoretical base of the kinetics estimation of the thermal decomposition

According to non-isothermal kinetic models, the commonly used kinetic equation of solid thermal decomposition is given as follows:

$$\frac{d\alpha}{dT} = \frac{A}{\beta} \exp\left(\frac{-E_a}{RT}\right) f(\alpha) \quad (1)$$

where α is fractional extent of reaction at time t, β the heating rate, E_a the apparent activation energy, $d\alpha/dT$ the rate of the reaction, A the pre-exponential factor, and $f(\alpha)$ is kinetic differential function. Its integral form is as follows:

$$G(\alpha) \int_0^{\alpha} \frac{d\alpha}{f(\alpha)} = \frac{A}{\beta} \int_0^{T} \exp\left(\frac{-E_a}{RT}\right) dT \quad (2)$$

The 15 reaction models and mechanism functions [24] were used to fit kinetics curves. The kinetic software from Netzsch was used in this analysis [25,26].

3. Results and discussion

The elemental analysis results for the mixed-ligand complexes were listed in Table 1. The results agree well with the given formulae of the compounds. The complexes are stable in air and soluble in most of organic solvents.

3.1. Thermal decomposition

3.1.1. [Ni(PMBP-PNH)$(Py)_3$]

The TG and DTG curves of the [Ni(PMBP-PNH)$(Py)_3$] are represented in Fig. 1. The decomposition of the mixed-ligand complex undergoes in four stages. Degradation of two pyridine molecules takes place in the first stage between 100 °C and 205 °C with a mass loss of 21.56% (Calc.: 21.51%). The maximum rate of mass loss is indicated by the DTG peak at 170 °C. The residue at the first stage was found to be [Ni(PMBP-PNH)Py] and the second stage between 205 °C and 360 °C corresponds to decomposition of the remaining pyridine molecule. The observed mass loss is 11.57% which is consistent with the theoretical value of 10.75%. With heating, the decomposition of the ligand (PMBP-PNH) was followed. Two well-separated peaks are displayed on the DTG curve, this indicates that the decomposition of the ligand (PMBP-PNH) divides into two steps. The third stage, which occurs in the temperature range 360–425 °C with a DTG peak at 403 °C, corresponding to the decomposition of the –Ph–NO_2 group, the observed mass loss (16.23%) is roughly coincide with the calculated value (16.60%). The fourth stage, occurs between 425 °C and 540 °C, corresponding to the further decomposition of the ligand, the mass loss (39.67%) is as against the theoretical value (40.97%). The maximum rate of mass loss is indicated by the DTG peak at 453 °C. The final residue, estimated as nickel oxide, has the observed mass 10.90% as against the calculated value of 10.16%.

The decomposition procedure can also be demonstrated by the crystal structure of the complex (Fig. 2) [22]. With regard to the bond distances, the Ni–N (pyridine) (Ni–N6, Ni–N7 and Ni–N8) distances are longer than other coordinating bond lengths (Table 2). In theory, these bonds are less stable and easy to be broken down. Therefore, the pyridine molecules were considered to be expelled before the degradation of the PMBP–PNH anion. Among the three pyridine molecules, Ni–N7 and Ni–N8 bond lengths (2.159 (2), 2.194 (2) Å) are longer than Ni–N6 bond length (2.088 (2) Å), indicating that the bond strengths of pyridyl nitrogen coordinated to

Table 1
The elemental analyses for the mixed-ligand complexes

Compound	Formula weight	Found(Calcd.) (%)		
		C (%)	H (%)	N (%)
[Ni(PMBP-PNH)$(Py)_3$]	735.42	63.86(63.70)	4.21(4.39)	14.94(15.24)
[Ni(PMBP-PNH)Py]	577.22	60.76(60.34)	3.57(3.84)	13.83(14.56)
[Cu(PMBP-PNH)Py]	582.08	59.78(59.84)	3.89(3.81)	13.95(14.44)

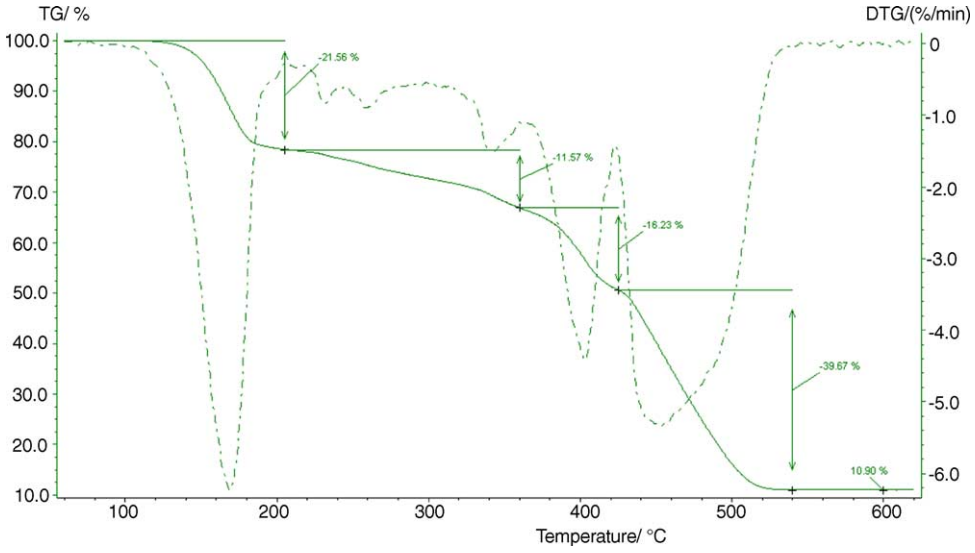

Fig. 1. The TG-DTG curves of [Ni(PMBP-PNH)Py_3]. Scanning rate 10 °C min^{-1}. (—) TG curve, (-···) DTG curve.

Ni(II) are different and Ni–N6 is stronger than Ni–N7 and Ni–N8. Thus, Ni–N6 bond was considered to be broken down following Ni–N7 and Ni–N8 bonds. The TG curve shows that two pyridine molecules were lost first and the removal of the remaining pyridine molecule was followed.

Therefore, the thermal decomposition process of [Ni(PMBP-PNH)$(Py)_3$] complex can be expressed by the following scheme:

$$[Ni(PMBP\text{-}PNH)(Py)_3] \rightarrow [Ni(PMBP\text{-}PNH)(Py)] \rightarrow [Ni(PMBP\text{-}PNH)] \rightarrow NiO$$

3.1.2. [Ni(PMBP-PNH)Py]

The typical TG-DTG curves of [Ni(PMBP-PNH)Py] are shown in Fig. 3. From the TG curve, decomposition starts at 200 °C and shows almost a continuous weight loss in the temperature range of 200–560 °C. Based on the percentages of weight losses, the DTG curve and the complexation sustainment, three-step decomposition is proposed for this complex. The first stage starts at 200 °C and ends at 358 °C. The observed mass loss (14.65%) is attributed to the decomposition of one pyridine molecule (theoretical mass loss: 13.70%). The second stage starts at 358 °C and ends at 428 °C, the corresponding mass loss (21.17%) is due to the degradation of the –Ph–NO_2 group of the PMBP-PNH anion, which is in well agreement with the calculated value (21.15%). The DTG peak corresponding to this stage is 403 °C. The third stage, which occurs in the temperature range 428–560 °C with a DTG peak at 457 °C, corresponding to the decomposition of the remaining part of the ligand, the observed mass loss (50.62%) coincides with the theoretical value (52.20%). The final residue, estimated as nickel oxide, has the observed mass 13.26% as against the calculated value of 12.94%.

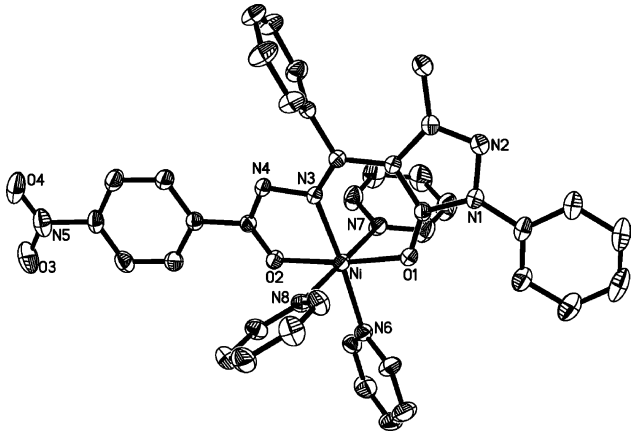

Fig. 2. The molecular structure of [Ni(PMBP-PNH)$(Py)_3$].

3.1.3. [Cu(PMBP-PNH)Py]

The thermal model of decomposition of the complex is shown in Fig. 4 and it indicates that it is thermally stable up to 160 °C. The thermal decomposition takes place in two distinct stages. In the first stage between 160 °C to 278 °C, the co-ligand pyridine degrades as shown as one maximum in the DTG curve at 186 °C with a 13.58% mass loss (Calc.: 13.60%). The second stage is related to decomposition of the PMBP-PNH anion in the temperature range of 300–620 °C, accompanied by a mass loss of 72.01% (Calc.: 72.74%). In the light of the DTG curve and the mass loss,

Table 2
Partial bond distances of [Ni(PMBP-PNH)$(Py)_3$]

Bond	Bond distance (Å)	Bond	Bond distance (Å)
Ni—O1	2.0390(17)	Ni—O2	2.0467(17)
Ni—N3	1.9965(19)	Ni—N6	2.088(2)
Ni—N7	2.159(2)	Ni—N8	2.192(2)

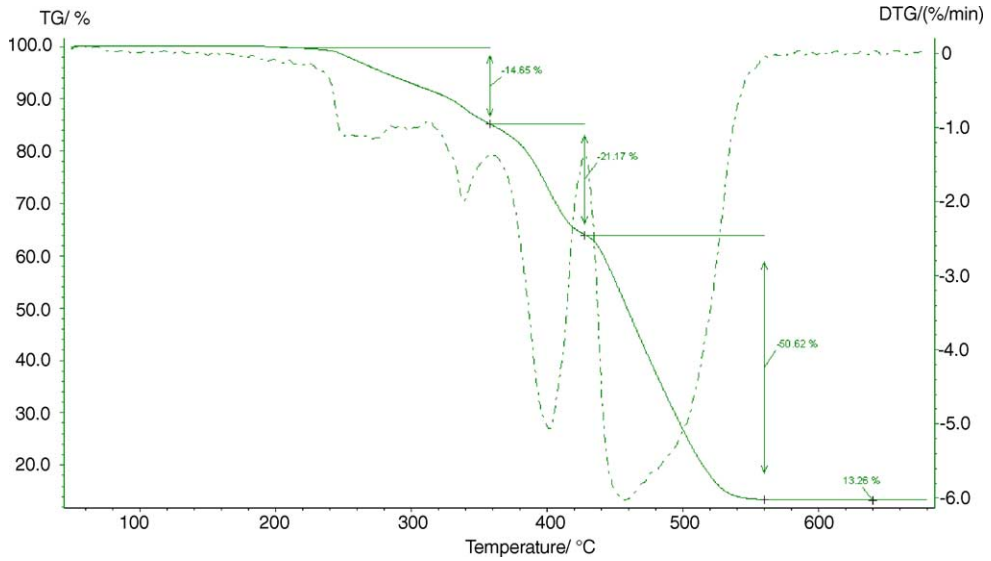

Fig. 3. The TG-DTG curves of [Ni(PMBP-PNH)Py]. Scanning rate 10 °C min^{-1}. (—) TG curve, (-···-) DTG curve.

we judge that decomposition of the ligand PMBP-PNH is a consecutive procedure and can't be separated as the former two complexes. Weight constancy is attained at around 580 °C. The end product, estimated as CuO, has the observed mass of 14.22% compared with the calculated value of 13.67%.

3.2. Kinetic analyses

The apparent activation energy of the decomposition process in non-isothermal conditions can be calculated by model-free isoconversional method [27–31]. The model-free kinetic analyses have the advantage of alleviating the need to select a specific kinetic model and hence any dependence on this choice. The Netzsch thermokinetics software package has the capacity to perform model-free kinetic analyses. According to our experience, the significance of the model-free analyses lies in its function as preliminary stage of non-linear regression. The determination of kinetic parameters by means of the non-linear regression is an iterative process. The preset of start values for the parameters is necessary. Here the model-free estimation of the activation energy means a great help for the non-linear regression for being able to deliver start values. Anyway the multi-step feature of a process often can only be detected from the dependence of the activation energy on the reaction degree.

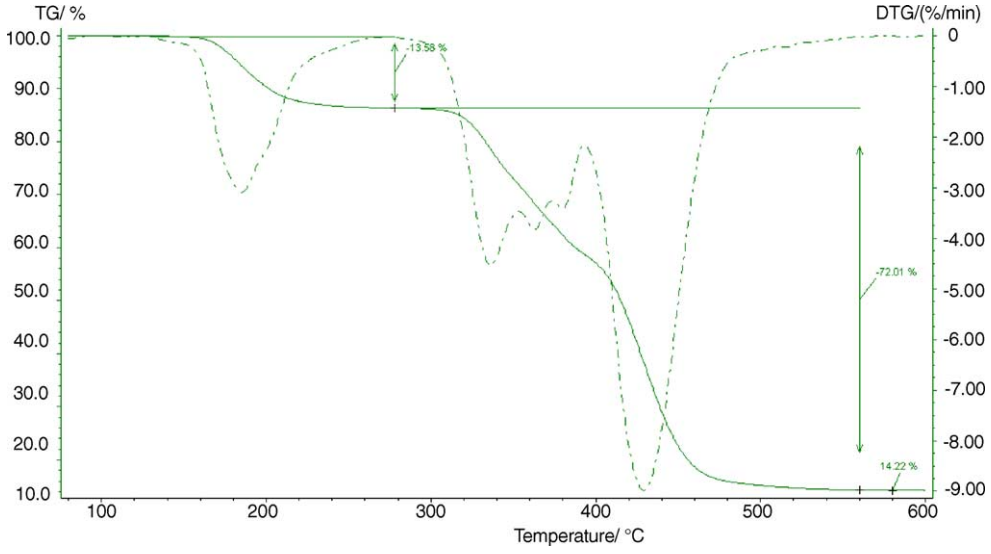

Fig. 4. The TG-DTG curves of [Cu(PMBP-PNH)Py]. Scanning rate 10 °C min^{-1}. (—) TG curve, (-···-) DTG curve.

Table 3
The optimized mechanism functions and kinetic parameters of three mixed-ligand complexes

Complexes	Steps	Mechanism	E_a (kJ mol^{-1})	log A (s^{-1})	Reaction order n	Exponent α	Correction coefficient
[Ni(PMBP-PNH)(Py)$_3$]	I	F1	115.48	11.70	1.00		0.99944
	II	Fn	89.81	6.05	3.50		0.99760
		Bna	100.05	6.93	0.91	1.42E−5	
		Fn	25.97	1.27	0.90		
	III	F1	240.1167	16.6092	1.00		0.99935
		Bna	138.1133	12.8156	0.6449	0.9483	
[Ni(PMBP-PNH)Py]	I	Fn	174.99	13.72	8.09		0.99898
		Bna	70.99	3.88	0.38	5.74E−6	
		Fn	112.14	8.44	0.72		
	II	F1	224.4565	15.4067	1.00		0.99950
		Bna	153.2284	10.8757	0.5750	0.8035	
[Cu(PMBP-PNH)Py]	I	Fn	467.5126	53.2179	4.7143		0.99941
		Fn	102.1752	9.4775	1.6953		
	II	Fn	264.98	20.56	2.00		0.99939
		Fn	125.45	6.91	0.72		

In this study, the Ozawa–Flynn–Wall model-free analyses and multivariate non-linear regression were applied to perform single and overall steps optimization. Kinetic parameters were given and the most probable mechanism functions were suggested (Table 3).

3.2.1. *Thermal kinetic TG-analysis of [Ni(PMBP-PNH)(Py)$_3$]*

The TG data for the first, second and third steps of this complex were analyzed by model-free method and non-linear fit to 15 mechanism functions.

Fig. 5 shows that the activation energy and pre-exponential factor of the first step are independent of the extend of conversion, the activation energy value is about 110 kJ mol^{-1}. This indicates that the first step is a single-step reaction. So single reaction mechanism was used to fit, the results were satisfied (Fig. 6).

Fig. 7 shows the activation energy was varied with the react conversion, this demonstrates that the second step reaction contains at least three steps. Therefore, three-step mechanism model was applied in the non-linear regression. The results were shown in Fig. 8 and Table 3.

We based on the variation of activation energy with the reaction fraction α for the third step of [Ni(PMBP-PNH)(Py)$_3$] (Fig. 9), and tried to use multi-step reaction mechanism model to fit. The results were shown in Fig. 10.

From Table 3, we see that the decomposition of first step adopted the one-step reaction model, and the reaction mechanism was F1, relevant E_a was 115.48 kJ mol^{-1}.The value was agree well with that from OFW analysis.

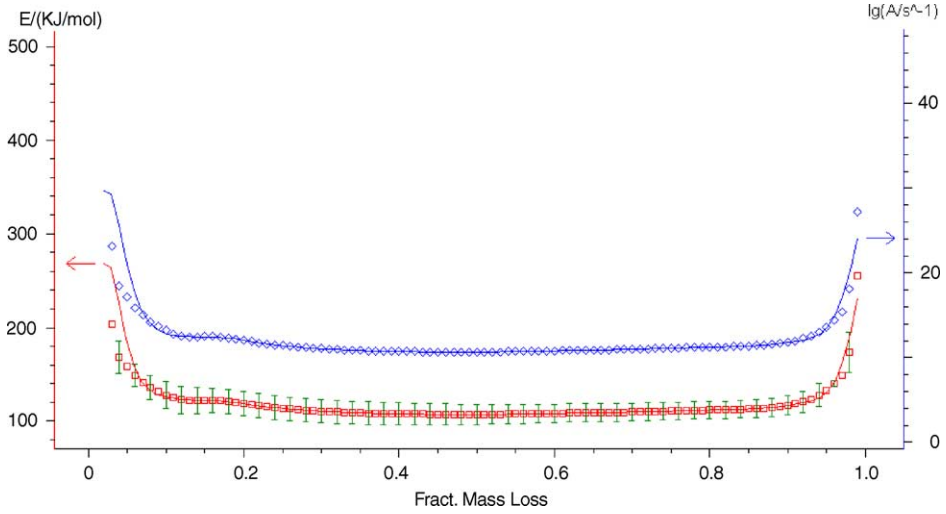

Fig. 5. A plot of E_a and log A as a function of α for the first step of [Ni(PMBP-PNH)(Py)$_3$] based on the OFW model-free method using TG results. The error limits specified by bars.

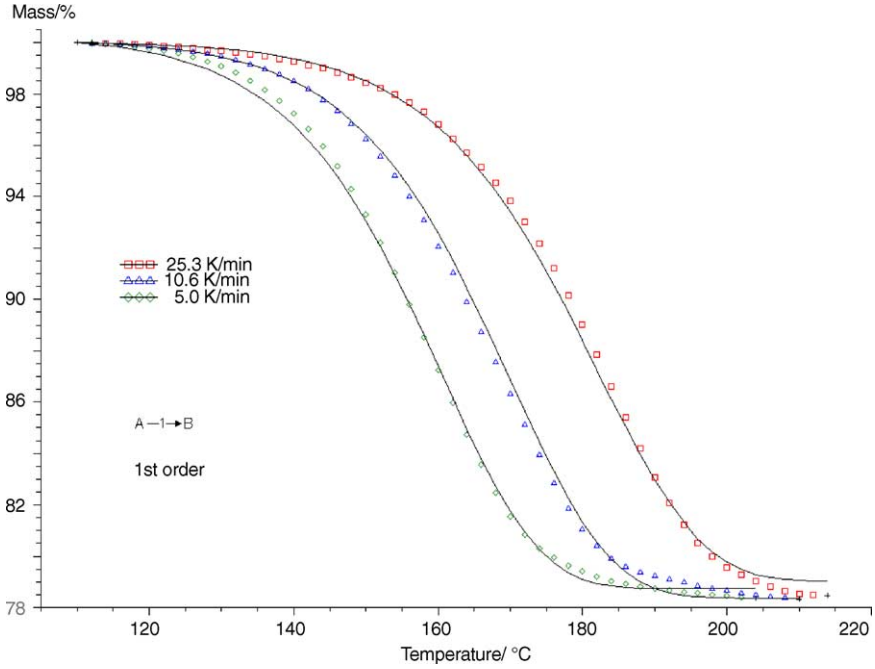

Fig. 6. Fit of the first step of the TG curve of [Ni(PMBP-PNH)(Py)$_3$], simulated with reaction type F1. Signs measured, (—) calculated.

The second step adopted A → B → C → D sequential reaction model and the reaction mechanism function was Fn–Bna–Fn. Compared with optimized multireaction mechanism of [Ni(PMBP-PNH)(Py)] (Fig. 12), the correction coefficient of the second step was not good. The third step adopted the A → B→ C reaction model and the mechanism function was F1–Bna. Single-step and multi-step reaction models were used to fit the fourth stage of the decomposition, unfortunately, a high quality of fit has not achieved.

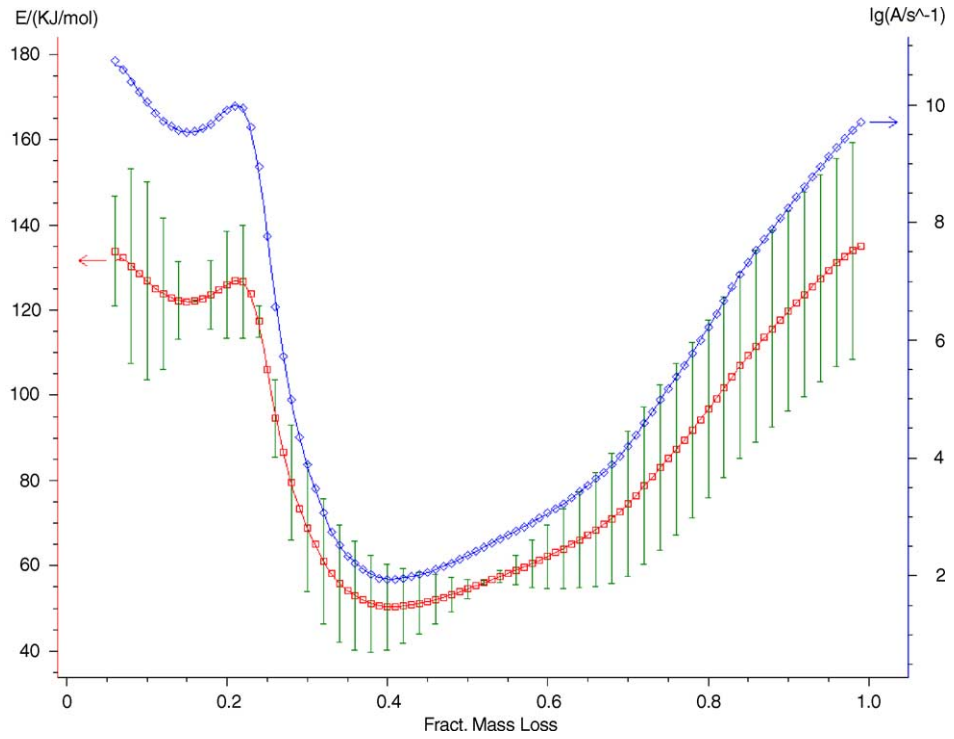

Fig. 7. A plot of E_a and log A as a function of α for the second step of [Ni(PMBP-PNH)(Py)$_3$] based on the OFW model-free method using TG results. The error limits specified by bars.

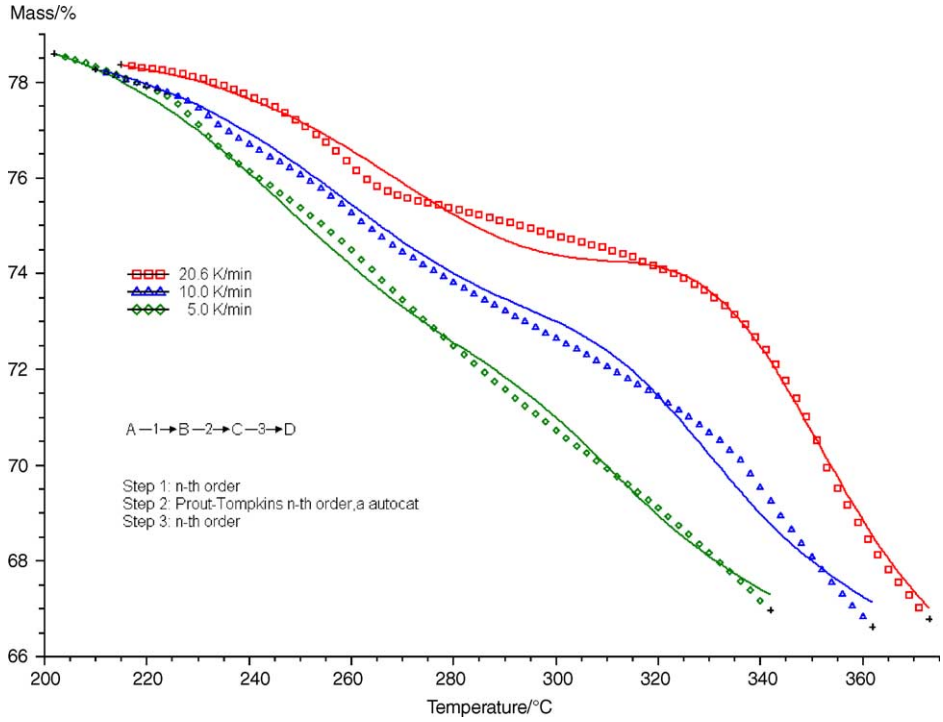

Fig. 8. Fit of the second step of the TG curve of [Ni(PMBP-PNH)$(Py)_3$]. Signs measured, (—) calculated.

3.2.2. Thermal kinetic TG-analysis of [Ni(PMBP-PNH)Py]

The stages of removal of pyridine molecule and –Ph–NO_2 group of PMBP-PNH were analyzed by the multivariate non-linear regression analysis. The start values for the parameters were taken from the OFW model-free analyses. The multireaction mechanisms were tested to fit the curves.

It is clear in Fig. 11 that the activation energy assumes a value of 210 kJ mol^{-1} at the beginning of the

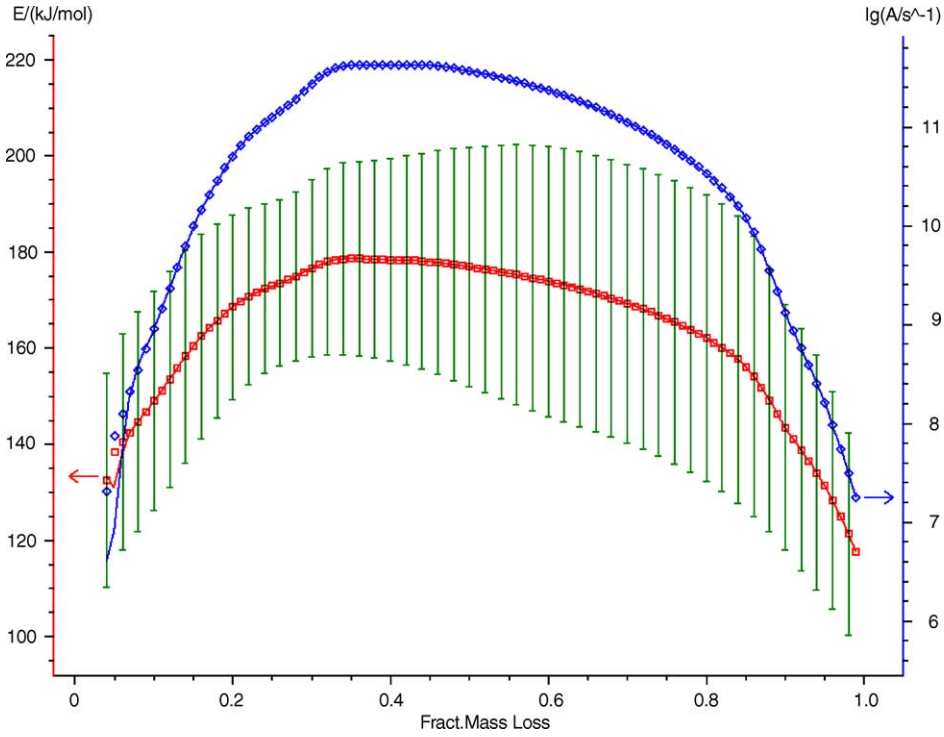

Fig. 9. A plot of E_a and log A as a function of α for the third step of [Ni(PMBP-PNH)$(Py)_3$] based on the OFW model-free method using TG results. The error limits specified by bars.

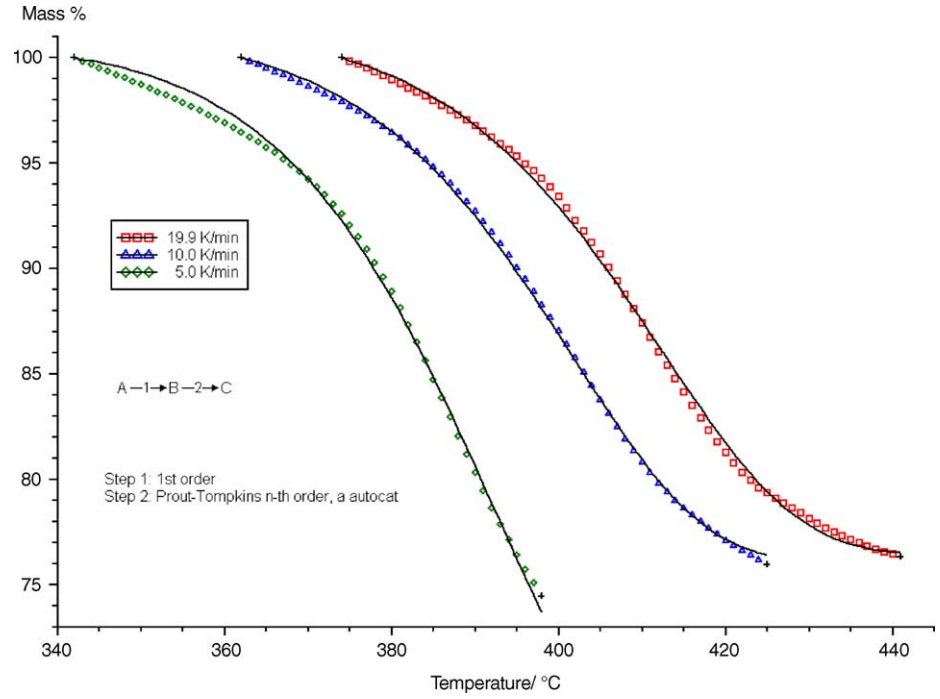

Fig. 10. Fit of the third step of the TG curve of [Ni(PMBP-PNH)(Py)$_3$]. Signs measured, (—) calculated.

decomposition and with increasing mass loss, drops to a value of 68 kJ mol^{-1}. At the end, the value ascends to about 240 kJ mol^{-1}. This dependence of the activation energy is an indication that the overall reaction contains three steps. Hence three-step mechanism model was used to fit it. The results were shown in Fig. 12.

Fig. 13 shows that the activation energy assumes a value of 235 kJ mol^{-1} at the beginning of reaction and at the end it drops to a value of 130 kJ mol^{-1}. This indicates

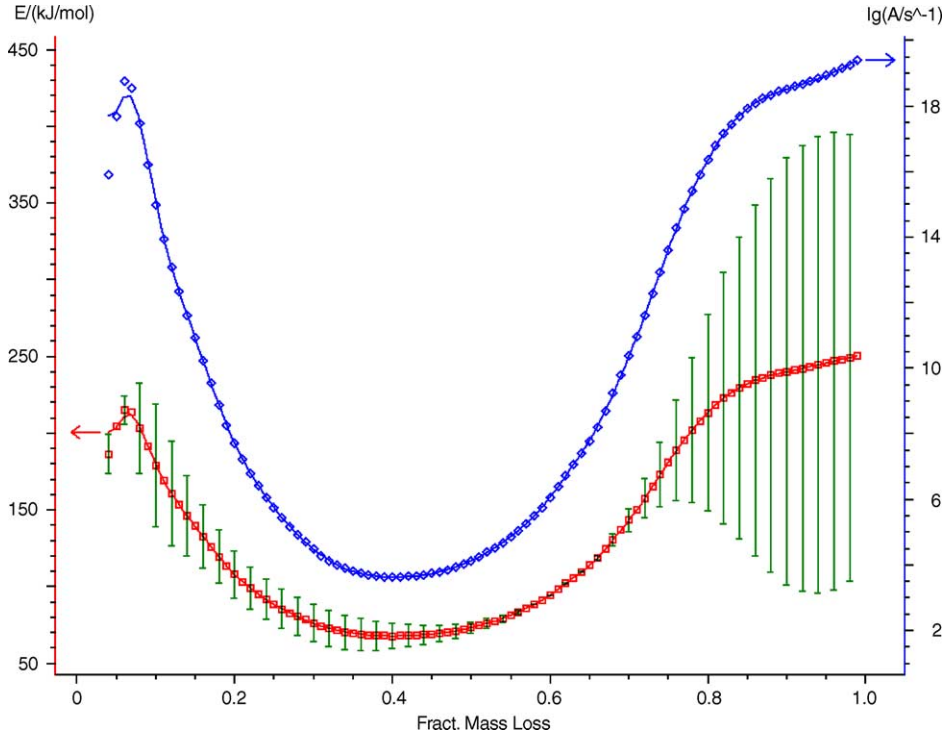

Fig. 11. Dependence of E_a and log A vs. α for the first step of [Ni(PMBP-PNH)(Py)] based on the OFW method.

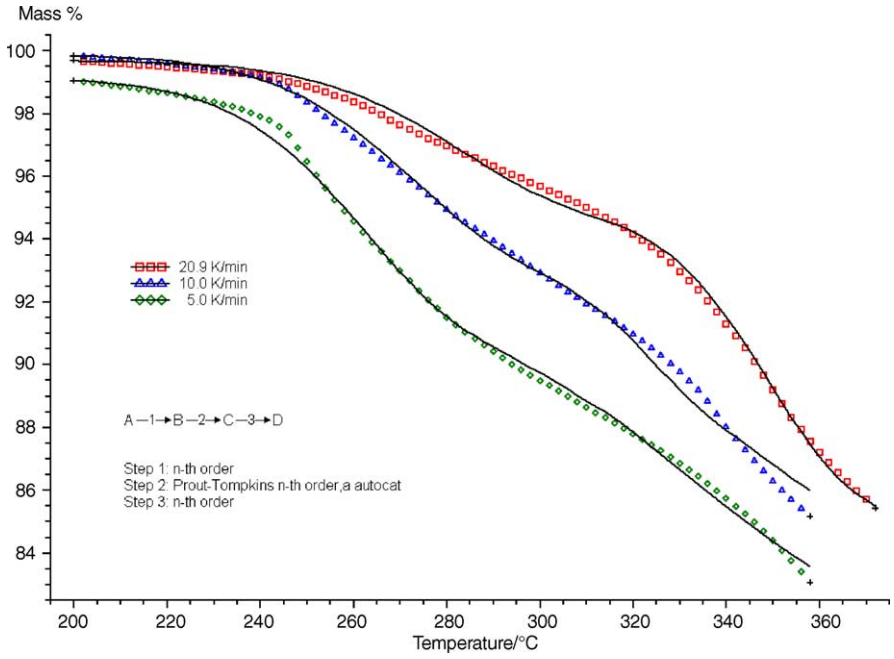

Fig. 12. Fit of the first step of the TG curve of [Ni(PMBP-PNH)(Py)]. Signs measured, (—) calculated.

that the decomposition reaction contains at least two steps. Presumably, the F1–Bna model was used to fit it, the results were satisfied (Fig. 14).

The optimized mechanism function of first step was $A \rightarrow B \rightarrow C \rightarrow D$ sequential reaction model, the mechanism function was Fn–Bna–Fn, relevant E_a were 174.99, 70.99 and 112.14 kJ mol^{-1}, and $\log A$ were 13.72, 3.88 and 8.44 s^{-1}. The second step adopted $A \rightarrow B \rightarrow C$ reaction model and the reaction mechanism function was F1–Bna. We tried to use single-step and multi-step mechanism model to fit the third stage of decomposition reaction, but the results were unsatisfied.

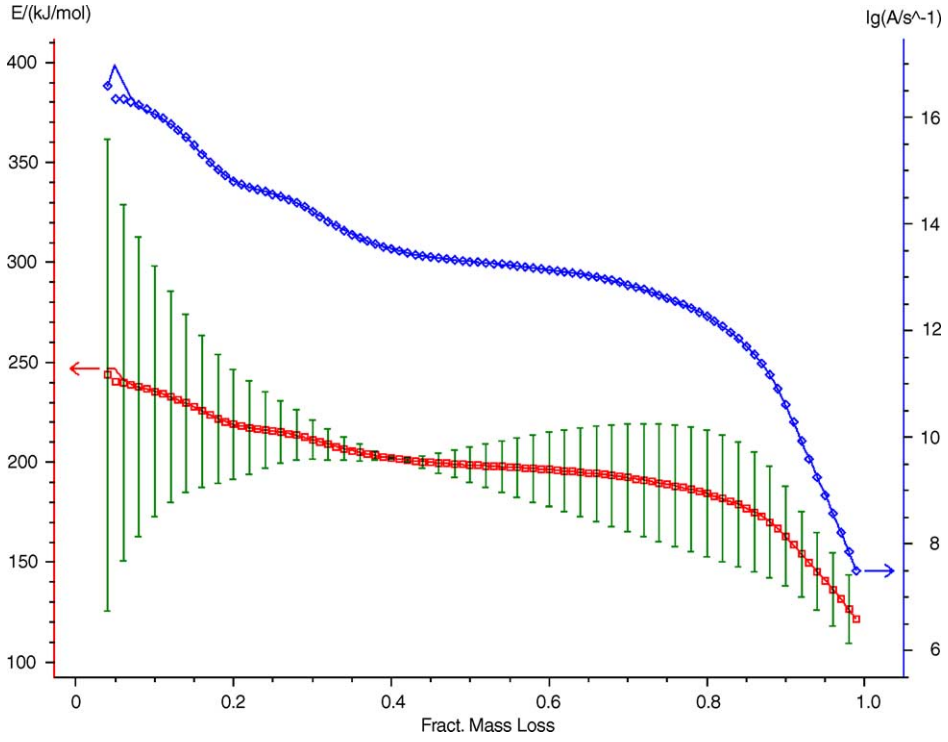

Fig. 13. Dependence of E_a and $\log A$ vs. α for the second step of [Ni(PMBP-PNH)(Py)] based on the OFW method.

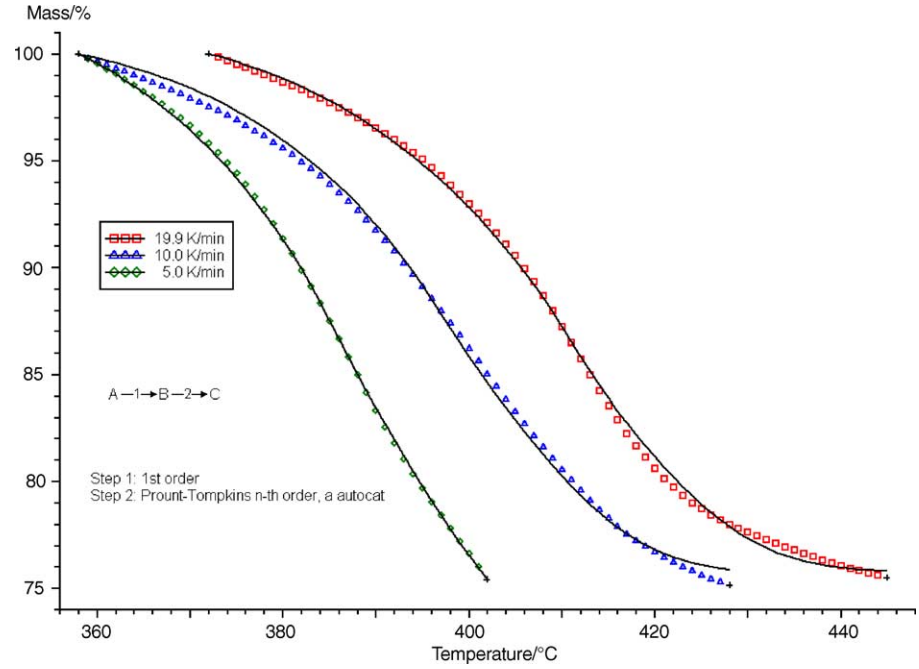

Fig. 14. Fit of the second step of the TG curve of [Ni(PMBP-PNH)(Py)]. Signs measured, (—) calculated.

3.2.3. *Thermal kinetic TG-analysis of [Cu(PMBP-PNH)Py]*

TG kinetics of the overall steps of [Cu(PMBP-PNH)Py] decomposition were fitted.

Fig. 15 shows the variation of E_a and $\log A$ as a function of α from the OFW analysis for the first step of the decomposition. E_a has a value about 460 kJ mol^{-1} in the rage of $0.02 < \alpha < 0.32$, with the increasing α, it drops to 125 kJ mol^{-1}. This indicates that the decomposition reaction contains two steps. So the Fn–Fn reaction model was used to fit it, the results were shown in Fig. 16.

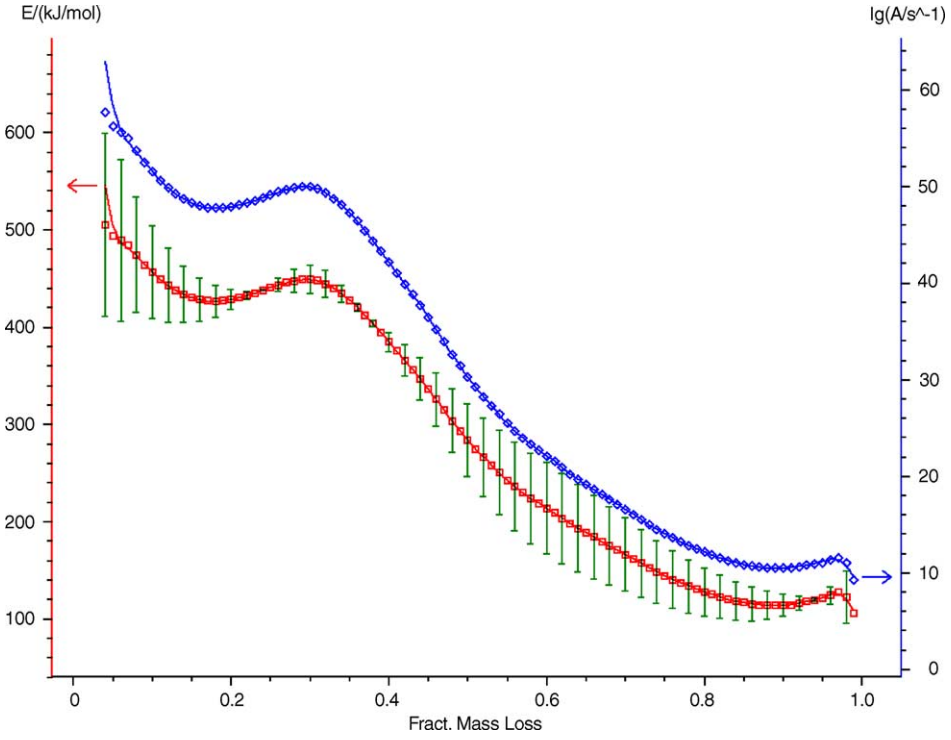

Fig. 15. A plot of E_a and $\log A$ as a function of α for the first step of [Cu(PMBP-PNH)(Py)] based on the OFW method using TG results.

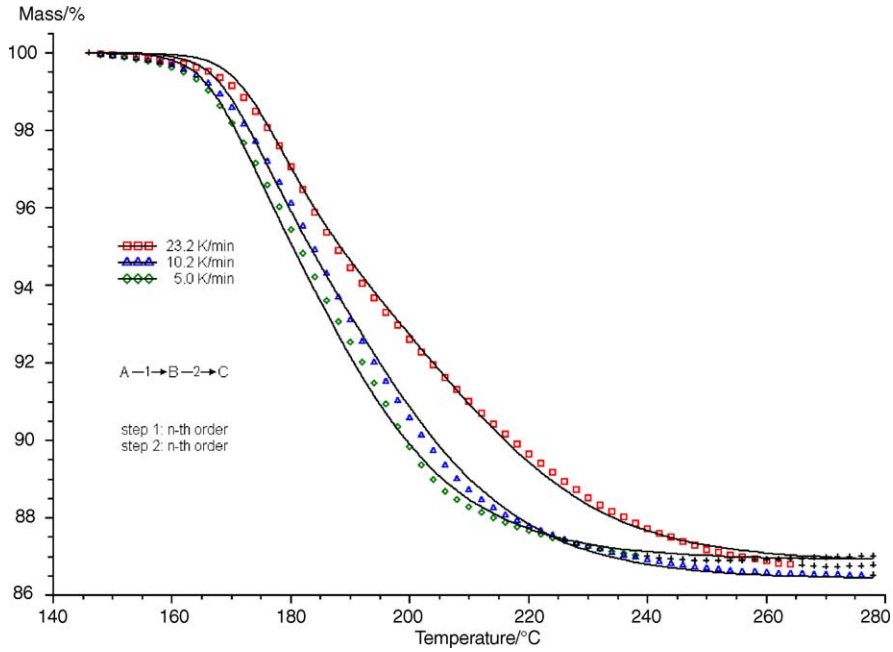

Fig. 16. The first step of the [Cu(PMBP-PNBH)Py] decomposition was the best fit to mechanism function. Signs measured, (—) calculated.

Fig. 17 shows the dependence of activation energy and of pre-exponential versus degree of reaction, the inconstant activation energy is serious indications of the presence of a multi-step process. Therefore, we tried to use multireaction mechanisms to fit. The results were satisfied (Fig. 18).

The results were shown in Figs. 16 and 18, respectively. The first step adopted $A \rightarrow B \rightarrow C$ reaction model, and the optimized mechanism function of this step was Fn–Fn, relevant Ea were 467kJ mol^{-1} and 102 kJ mol^{-1}. The second step also adopted $A \rightarrow B \rightarrow C$ sequential reaction, and the reaction mechanism function was Fn–Fn.

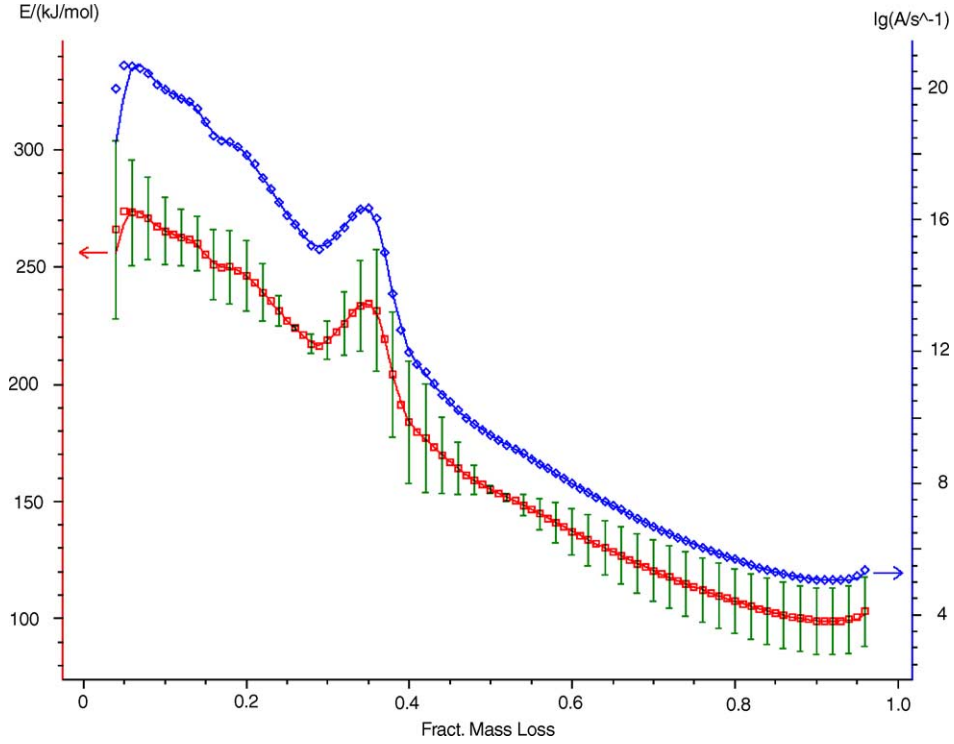

Fig. 17. A plot of E_a and log A as a function of α for the second step of [Cu(PMBP-PNH)(Py)] based on the OFW model-free method using TG results.

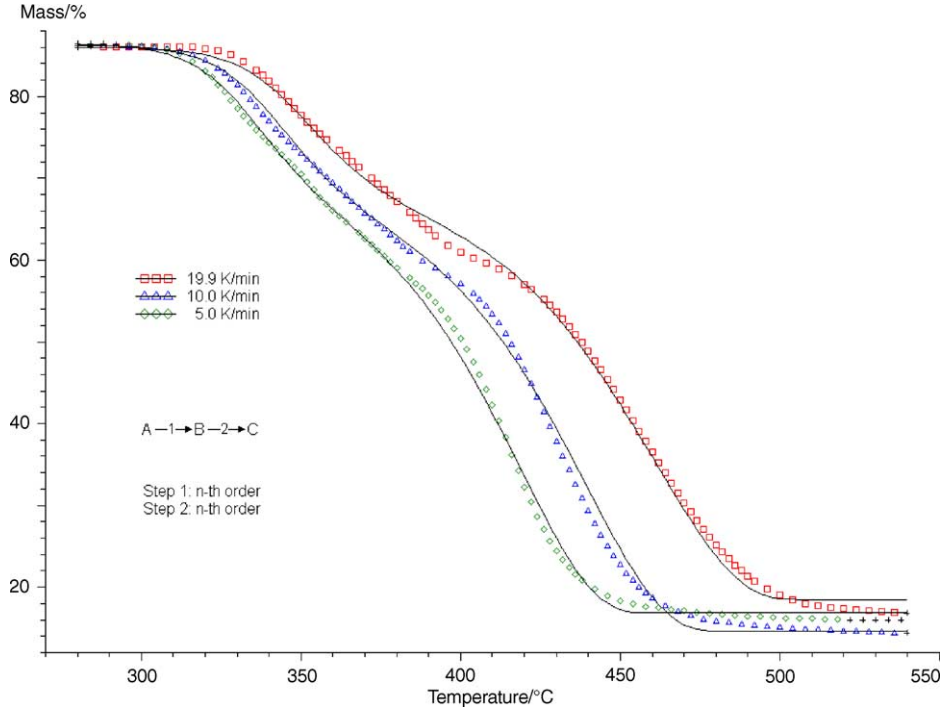

Fig. 18. The second step of the [Cu(PMBP-PNBH)Py] decomposition was the best fit to mechanism function. Signs measured, (—) calculated.

Acknowledgement

This work was supported by the National Natural Science Foundation of China (No. 20262005, 20366005).

References

[1] N. Raman, A. Kulandaisamy, A. Shunmugasundaram, K. Jeyasubramanian, Transition Met. Chem. 26 (2001) 131.
[2] T. Yoshikuni, J. Mol. Catal. A-Chem. 148 (1999) 285.
[3] B.A. Uzoukwu, P.U. Adiukwu, S.S. Al-Juaid, P.B. Hitchcock, J.D. Smith, Inorg. Chim. Acta 250 (1996) 173.
[4] Z.Y. Yang, R.D. Yang, F.S. Li, K.B. Yu, Polyhedron 19 (2000) 2599.
[5] W.F. Yang, S.G. Yuan, Y.B. Xu, Y.H. Xiao, K.M. Fang, J. Radioanal. Nucl. Chem. 256 (2003) 149.
[6] A.K. El-Sawaf, D.X. West, Transition Met. Chem. 23 (1998) 417.
[7] N. Kalarani, S. Sangeetha, P. Kamalakannan, D. Venkappayya, Russ. J. Coord. Chem. 29 (2003) 845.
[8] C. Pettinari, F. Marchetti, C. Santini, R. Pettinari, A. Drozdov, S. Troyanov, G.A. attiston, R. Gerbasi, Inorg. Chim. Acta 315 (2001) 88.
[9] F. Marchetti, C. Rettinar, R. Pettinari, A. Cingolani, D. Leonesi, A. Lorenzotti, Polyhedron 18 (1999) 3041.
[10] O.N. Kataeva, A.T. Gubaidullin, I.A. Litvinov, O.A. Lodochnikova, L.R. Islamov, A.I. Movchan, G.A. Chmutova, J. Mol. Struct. 610 (2002) 175.
[11] Y. Akama, A. Tong, Microchem. J. 53 (1996) 34.
[12] Y. Akama, A. Tong, N. Matsumoto, T. Ikeda, S. Tunaka, Vib. Spectrosc. 13 (1996) 113.
[13] M.F. Iskander, L. Sayed, A.F.M. Hefny, S.E. Zayan, J. Inorg. Nucl. Chem. 38 (1976) 2209.
[14] G.H. Havanur, V.B. Mahale, Indian J. Chem. 26A (1987) 1063.
[15] H. Adams, D.E. Fenton, G. Minardi, E. Mura, M. Angelo, Inorg. Chem. Commun. 3 (2000) 4.
[16] X.C. Tang, D.Z. Jia, K.B. Yu, X.G. Zhang, X. Xia, Z.Y. Zhou, J. Photochem. Photobiol. A: Chem. 134 (2000) 23.
[17] L. Liu, D.Z. Jia, Y.M. Qiao, Y.L. Ji, K.B. Yu, J. Chem. Crystallogr. 32 (2002) 255.
[18] L. Liu, D.Z. Jia, Y.L. Ji, K.B. Yu, J. Photochem. Photobiol. A: Chem. 154 (2003) 117.
[19] L. Liu, D.Z. Jia, Y.L. Ji, Synth. React. Inorg. Met. Org. Chem. 32 (2002) 739.
[20] L. Liu, D.Z. Jia, Y.M. Qiao, K.B. Yu, Chin. J. Chem. 20 (2002) 286.
[21] Y.L. Ji, L. Liu, D.Z. Jia, Y.M. Qiao, K.B. Yu, J. Chem. Crystallogr. 32 (2002) 505.
[22] L. Zhang, L. Liu, D.Z. Jia, K.B. Yu, Struct. Chem. 15 (2004) 327.
[23] Y.L. Ji, L. Liu, D.Z. Jia, K.B. Yu, Chin. J. Struct. Chem. 21 (2002) 553.
[24] D. Dollimore, P. Tong, K.S. Alexander, Thermochim. Acta 282–283 (1996) 13.
[25] J. Opfermann, J. Therm. Anal. Calorim. 60 (2000) 641.
[26] J. Li, F.X. Zhang, Y.W. Ren, Y.Q. Hun, Y.F. Nan, Thermochim. Acta 406 (2003) 77.
[27] H.L. Friddman, J. Polym. Sci. 6 (1965) 183.
[28] T. Ozawa, Bull. Chem. Soc. Jpn. 38 (1965) 1881.
[29] J.H. Flynn, L.A. Wall, J. Polym. Sci. 4 (1966) 323.
[30] S. Vyazovkin, Thermochim. Acta 211 (1992) 181.
[31] S. Vyazovkin, Int. Rev. Phys. Chem. 19 (2000) 45.